Interface phonons in the active region of a quantum cascade laser

Gangyi Xu and Aizhen Li
State Key Laboratory of Functional Materials for Informatics, Shanghai Institute of Microsystem and Information Technology, Chinese Academy of Sciences, 865 Changning Road, Shanghai 200050, People's Republic of China
(Received 10 June 2004; revised manuscript received 21 March 2005; published 3 June 2005)

We consider the electrostatic potential and the dispersion relation of interface phonons in the active region of the quantum cascade laser. We propose a model which takes into account all the stages of the active region as a whole and the interaction between the stages. Our model agrees with the model for the finite superlattice [Phys. Rev. B **32**, 6544 (1985)], but can apply to a more general case in which each repeated stage is allowed to contain an arbitrary number of layers. Numerical calculations show that the interface phonons in the active region can be classified into bulk modes and surface modes. The dispersion curves of bulk modes form a series of subbands, and the electrostatic potentials propagate in the interior of the active region in an oscillating way. The dispersion curves of the surface modes are located in the gaps between the subbands of the bulk modes, and the electrostatic potentials are seen to be localized at the interface between the active region and the waveguide layer. Our calculations indicate that the distribution of phonon potential in different stages is significantly different. We also demonstrate that the transition matrix model cannot be used directly to deal with interface phonons in the active region, since it cannot keep the electrostatic potential continuous at the interface between adjacent stages. Our results are helpful to the design of quantum cascade lasers and other intersubband lasers.

DOI: 10.1103/PhysRevB.71.235304 PACS number(s): 68.35.Ja, 63.22.+m, 63.20.Kr, 42.55.Px

I. INTRODUCTION

The quantum cascade laser (QCL) is an important semiconductor laser source from the point of view of basic research and potential applications. Extremely impressive development has been made since the announcement in 1994.[1–7] The QCL is an electrically pumped diode laser based on intersubband transitions in the active region consisting of many identical stages. Each stage is actually a coupled multiple quantum well structure. As is well known, the scattering between electrons and longitudinal optical (LO) phonons is the most convenient and effective way to modify the lifetime of the electrons in laser states and hence to control the population inversion.[8–10] More importantly, the scattering with interface optical (IF) phonons has been proved to be the most important process that dominates the lifetime of the electrons.[11–13] Therefore, a precise description of IF phonons is of primary importance.

In the case of multiple heterostructures, optical phonons can be strongly influenced by the presence of heterointerfaces and their interaction with two-dimensional confined electrons will be significantly modified compared with the three-dimensional case. The properties of IF phonons in heterostructures have been theoretically studied by both macroscopic and microscopic approaches.[14–18] Recently, Yu *et al.* developed a transfer matrix model to study the IF phonons in multiple heterostructures.[19] This method is deduced in the framework of dielectric continuum theory and proved to be a great success since, compared with the detailed microscopic calculations, it provides a comparable accurate result and considerably saves computation time.[20–22] Therefore, at present, the transfer matrix model is commonly used to calculate the propagation of IF phonons in the active region of QCLs.[23–25] However, since the active region usually consists of dozens of stages and hence contains hundreds of heterointerfaces, it is difficult to study the IF phonons in the whole structure by the transfer matrix model. For the sake of simplicity, the model is usually used to calculate the propagation of the IF phonons in an isolated stage and it is assumed that in all stages the propagations of the IF phonons are completely the same.

Whether this assumption holds true is very important in the design of QCLs. Therefore, we discuss two questions:

(1) Considering the IF phonon, can we treat each stage as an isolated system and neglect the interaction between the stages?

(2) Is the propagation of IF phonon identical in each stage?

This paper studies these questions by developing a modified model and calculating in detail the properties of IF phonons. Our model, based on dielectric continuum theory, takes into account all the stages and the interaction between them. Typically, the active region consists of dozens of or even more than one hundred identical stages, each of which usually contains several or more than ten layers. Each stage is usually dozens of nanometers thick. On the one hand, the amplitudes of phonon potentials in the layers of the same stage can be related to each other by a series of matrices, as the transfer matrix model already shows. On the other hand, the stacking of so many stages indicates the periodicity in the interior of the active region. This enables us to treat the propagation of phonon potential along the stages by Bloch's theorem.[26,27] Based on the analysis mentioned above, we can derive a general form of the phonon potential. Next, by imposing the boundary conditions we can determine numerically the phonon potentials and the dispersion relations. Under the dielectric continuum theory, the polarization field, the electric field, and the electrostatic potential caused by the optical phonon can be deduced from each other by the classical electrostatic equations. In this work, we consider elec-

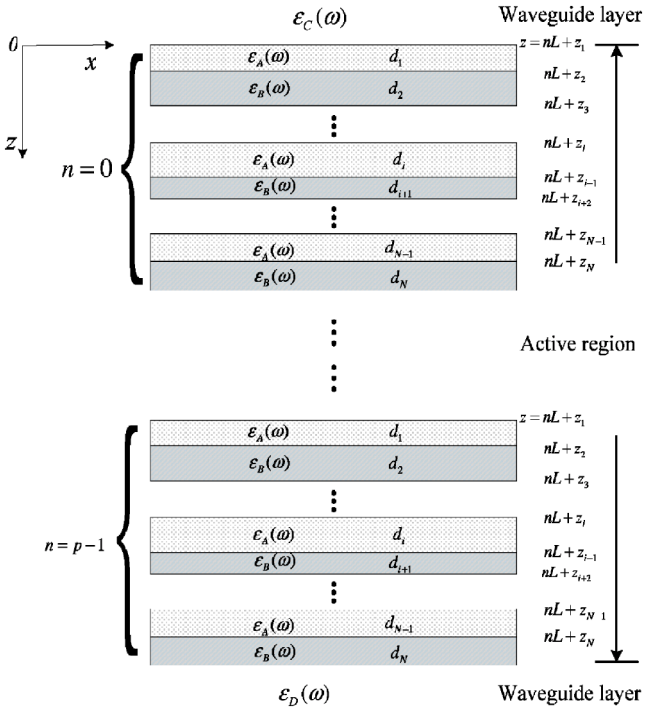

FIG. 1. Schematic figure of the active region structure. The active region has a total of p stages. Each stage is composed of alternating layers of material A and B, and contains N layers with the thickness of each layer being d_i $(i=1,2,\ldots N)$, $d_i \equiv z_{i+1}-z_i$. The active region is sandwiched between the waveguide layers C and D.

trostatic potential instead, since it can be directly used to calculate the electron-phonon scattering rate.

The paper is organized as follows. In Sec. II we propose our model to establish a general form of the electrostatic potential of IF phonons. An implicit dispersion relation is derived for IF phonons in the active region sandwiched between the waveguide layers. We also prove the consistency between our model and the model for finite superlattice.[27] In Sec. III, as an example, properties of the IF phonons in a practical QCL structure are studied by using the transfer matrix model and our model, respectively. Numerical results demonstrate the defect of the transfer matrix model, and show unique properties of IF phonons exposed by our model. The conclusion is given in Sec. IV.

II. THEORY

In this section we present the general solution to the electrostatic potential of IF phonons in an active region structure. After that, an implicate dispersion relation for IF phonons is derived. Figure 1 shows the structure under consideration. The active region has p stages in total and is sandwiched between waveguide layers of material C and D. Each stage, which consists of alternating layers of material A and B, contains N layers. The thickness of each layer is d_i $(i=1,2,\ldots,N)$. The repetition period is $L=\Sigma_{i=1}^{N} d_i$. The dielectric constant of each material is a function of frequency, $\varepsilon_i=\varepsilon_i(\omega)$ $(i=A,B,C,D)$. We establish the coordinates with the z axis normal to each A-B interface and the x axis parallel to the same, and the origin of the z axis is set at the interface between the waveguide layer (material C) and the active region. The electrostatic potential $\phi(\mathbf{r},t)$ must satisfy Laplace's equation everywhere, $\nabla^2\phi(\mathbf{r},t)=0$. The translational invariance in the x and y directions enables the electrostatic potential to be characterized by a wave vector $\mathbf{k}$ parallel to the interface. Without loss of generality, we assume that each material is isotropic, and define $\mathbf{k}$ parallel to the x axis. Under this assumption the electrostatic potential of the IF phonon has the form $\phi(\mathbf{r},t)=e^{i(kx-\omega t)}\Phi(z)$, and $\Phi(z)$ satisfies the equation

$$\left[\frac{d^2}{dz^2}-k^2\right]\Phi(z)=0, \tag{1}$$

where $k=|\mathbf{k}|$ is the amplitude of the wave vector in the in-plane direction. The most general solution to Eq. (1) is a linear combination of exponentially decaying and exponentially growing spatial functions:

$$\Phi(z)=A_+e^{+kz}+A_-e^{-kz}. \tag{2}$$

First, in waveguide layers C $(z\leqslant 0)$ and D $(z\geqslant pL)$, we have

$$\Phi(z)=Ce^{kz}, \quad z\leqslant 0 \tag{3a}$$

$$\Phi(z)=De^{-kz}, \quad z\geqslant pL. \tag{3b}$$

Since the interior of the active region is periodic we can invoke Bloch's theorem. In the ith layer of the nth stage, $nL+z_i\leqslant z\leqslant nL+z_{i+1}$ (here $d_i\equiv z_{i+1}-z_i$), the electrostatic potential is

$$\begin{aligned}\Phi_{n,i}(z)=&e^{-\gamma nL}(A_{i,+}e^{k(z-nL-z_i)}+A_{i,-}e^{-k(z-nL-z_i)})\\&+e^{\gamma nL}(A'_{i,+}e^{k(z-nL-z_i)}+A'_{i,-}e^{-k(z-nL-z_i)}).\end{aligned} \tag{3c}$$

Here, the constant γ, arising due to the periodicity in the z direction in the active region, can be regarded as a wave vector that characterizes the electrostatic potential propagating along the z direction. Equation (3c) shows $\Phi_{n,i}(z)$ can be expressed as a sum of two terms. Each term is essentially composed of a surface-wave electrostatic potential in each layer multiplied by an envelope function ($e^{-\gamma nL}$ or $e^{-\gamma(p-n)L}$) that relates the amplitude of one stage to another. In Eq. (3c) factors of $e^{-\gamma pL}$ are incorporated in the coefficients $A'_{i,+}$ and $A'_{i,-}$. We can find Eq. (3c) is consistent with Eq. (2), the most general form of the IF phonon potential. The terms $e^{k(z-nL-z_i)}$ and $e^{-k(z-nL-z_i)}$ allow the solution to have the characteristics of IF phonon. The IF phonon described by the solution is located in the vicinity of interfaces and decays away from them. All the coefficients and the constant γ can be found just by taking the boundary conditions and the attenuation condition into account. The boundary conditions require that the electrostatic potential and the tangential component of the electric field should be continuous, i.e., $\Phi(z)$ and $\varepsilon(\omega)[\partial\Phi(z)/\partial z]$ must be continuous at each interface. In addition, the attenuation condition requires $\lim_{z\to\pm\infty}\Phi(z)=0$.

According to the property of γ, IF phonons can be classified into two types of modes. If γ has a real part, the envelope functions $e^{-\gamma nL}$ and $e^{-\gamma(p-n)L}$ tend to localize near the

top and bottom interface of the whole structure, and the corresponding electrostatic potential shows the characteristics of a surface wave. Therefore, we call these IF modes the "surface modes." However, if γ is purely imaginary, the electrostatic potential will propagate in an oscillating manner in the active region and shows the characteristics of bulk wave. We call these IF modes the "bulk modes."

The boundary conditions are treated in three steps. We deal with the boundary conditions at the interfaces between the layers in one stage, at the interfaces between two adjacent stages, and at the interfaces between the active region and waveguide layers. When the solution $\Phi(z)$ simultaneously satisfies the conditions mentioned above, it should simultaneously satisfy the boundary conditions at all the interfaces in the system we consider.

We first deal with the boundary conditions in one stage. At the interface between the ith layer and the $(i+1)$th layer in the nth stage, $z=nL+z_{i+1}$, continuity of $\Phi(z)$ gives us

$$A_{i,+}e^{kd_i} + A_{i,-}e^{-kd_i} = A_{i+1,+} + A_{i+1,-}, \tag{4}$$

$$A'_{i,+}e^{kd_i} + A'_{i,-}e^{-kd_i} = A'_{i+1,+} + A'_{i+1,-}, \tag{5}$$

and continuity of $\varepsilon(\omega)\,[\partial\Phi(z)/\partial z]$ gives us

$$\varepsilon_i(A_{i,+}e^{kd_i} - A_{i,-}e^{-kd_i}) = \varepsilon_{i+1}(A_{i+1,+} - A_{i+1,-}), \tag{6}$$

$$\varepsilon_i(A'_{i,+}e^{kd_i} - A'_{i,-}e^{-kd_i}) = \varepsilon_{i+1}(A'_{i+1,+} - A'_{i+1,-}), \tag{7}$$

where ε_i refers to the dielectric function of the material of ith layer $[\varepsilon_i=\varepsilon_A(\omega)$ or $\varepsilon_B(\omega)]$. Equations (4)–(7) can be written compactly in a matrix form as follows:

$$\begin{pmatrix} A_{i+1,+} \\ A_{i+1,-} \end{pmatrix} = G_i \begin{pmatrix} A_{i,+} \\ A_{i,-} \end{pmatrix}, \tag{8}$$

$$\begin{pmatrix} A'_{i+1,+} \\ A'_{i+1,-} \end{pmatrix} = G_i \begin{pmatrix} A'_{i,+} \\ A'_{i,-} \end{pmatrix}. \tag{9}$$

The transfer matrix G_i is defined as

$$G_i = \frac{1}{2}\begin{pmatrix} 1 & 1 \\ 1 & -1 \end{pmatrix}\begin{pmatrix} e^{kd_i} & e^{-kd_i} \\ (\varepsilon_i/\varepsilon_{i+1})e^{kd_i} & -(\varepsilon_i/\varepsilon_{i+1})e^{-kd_i} \end{pmatrix}, \tag{10}$$

where the transfer matrix G_i relates the coefficients of electrostatic potential in ith and $(i+1)$th layers. By applying the chain rule, coefficients of electrostatic potential in the layers of the same stage can be related to each other by a series of transfer matrices. For example, in the first layer and the last (nth) layer of one stage, the coefficients have the relations as follows:

$$\begin{pmatrix} A_{N,+} \\ A_{N,-} \end{pmatrix} = G_{N-1}\cdots G_i \cdots G_1 \begin{pmatrix} A_{1,+} \\ A_{1,-} \end{pmatrix}, \tag{11}$$

$$\begin{pmatrix} A'_{N,+} \\ A'_{N,-} \end{pmatrix} = G_{N-1}\cdots G_i \cdots G_1 \begin{pmatrix} A'_{1,+} \\ A'_{1,-} \end{pmatrix}. \tag{12}$$

Next, we impose the boundary conditions at the interface between the nth stage and the $(n+1)$th stage, $z=nL+z_{N+1}=(n+1)L+z_1=(n+1)L$ (in our coordinates $z_1\equiv 0$), to obtain

$$e^{-\gamma nL}[A_{N,+}e^{kd_N} + A_{N,-}e^{-kd_N}] + e^{\gamma nL}[A'_{N,+}e^{kd_N} + A'_{N,-}e^{-kd_N}] = e^{-\gamma(n+1)L}[A_{1,+} + A_{1,-}] + e^{\gamma(n+1)L}[A'_{1,+} + A'_{1,-}] \tag{13}$$

and

$$\varepsilon_N\{e^{-\gamma nL}[A_{N,+}e^{kd_N} - A_{N,-}e^{-kd_N}] + e^{\gamma nL}[A'_{N,+}e^{kd_N} - A'_{N,-}e^{-kd_N}]\} = \varepsilon_1\{e^{-\gamma(n+1)L}[A_{1,+} - A_{1,-}] + e^{\gamma(n+1)L}[A'_{1,+} - A'_{1,-}]\}. \tag{14}$$

Similarly, Eqs. (13) and (14) can be expressed in matrix form,

$$e^{-\gamma L}\begin{pmatrix} A_{1,+} \\ A_{1,-} \end{pmatrix} = G_N \begin{pmatrix} A_{N,+} \\ A_{N,-} \end{pmatrix}, \tag{15}$$

$$e^{\gamma L}\begin{pmatrix} A'_{1,+} \\ A'_{1,-} \end{pmatrix} = G_N \begin{pmatrix} A'_{N,+} \\ A'_{N,-} \end{pmatrix}. \tag{16}$$

We combine the boundary conditions at the interfaces between layers in one stage and those at the interfaces between two adjacent stages by substituting Eqs. (11) and (12) into Eqs. (15) and (16), and find

$$e^{-\gamma L}\begin{pmatrix} A_{1,+} \\ A_{1,-} \end{pmatrix} = M \begin{pmatrix} A_{1,+} \\ A_{1,-} \end{pmatrix}, \tag{17}$$

$$e^{\gamma L}\begin{pmatrix} A'_{1,+} \\ A'_{1,-} \end{pmatrix} = M \begin{pmatrix} A'_{1,+} \\ A'_{1,-} \end{pmatrix}, \tag{18}$$

where

$$M = G_N G_{N-1}\cdots G_1. \tag{19}$$

Equations (17) and (18) admit a solution only if the determinant of the coefficient matrix vanishes. Both equations yield the same condition on γ as follows:

$$\det[M - e^{-\gamma L}E] = 0, \tag{20}$$

where E is a unit matrix. When each stage contains only two layers ($N=2$), the active region will be simplified to be a finite superlattice. In this case, Eq. (20) has a more explicit expression as follows:

$$\cosh(\gamma L) = \cosh(kd_2)\cosh(kd_1) + \frac{1}{2}\left(\frac{\varepsilon_A}{\varepsilon_B} + \frac{\varepsilon_B}{\varepsilon_A}\right)\sinh(kd_2)\sinh(kd_1). \tag{21}$$

The above equation completely agrees with Eq. (33) in Ref. 27, which is the condition on γ in the interior of a finite superlattice.

Finally, we treat the boundary conditions at the interfaces between the active region and waveguide layers. At $z=0$, we obtain

$$C = A_{1,+} + A_{1,-} + A'_{1,+} + A'_{1,-}, \tag{22}$$

$$\varepsilon_C C = \varepsilon_A(A_{1,+} - A_{1,-} + A'_{1,+} - A'_{1,-}). \tag{23}$$

Similarly, at the interface between active region and material D, $z=pL$, we find

$$De^{-kpL} = e^{-\gamma(p-1)L}[A_{N,+}e^{kd_N} + A_{N,-}e^{-kd_N}] + e^{\gamma(p-1)L}[A'_{N,+}e^{kd_N} + A'_{N,-}e^{-kd_N}], \quad (24)$$

and

$$-\varepsilon_D De^{-kpL} = \varepsilon_N\{e^{-\gamma(p-1)L}[A_{N,+}e^{kd_N} - A_{N,-}e^{-kd_N}] + e^{\gamma(p-1)L}[A'_{N,+}e^{kd_N} - A'_{N,-}e^{-kd_N}]\}. \quad (25)$$

By substituting Eqs. (13) and (14) into (24) and (25), we find

$$De^{-kpL} = e^{-\gamma pL}[A_{1,+} + A_{1,-}] + e^{\gamma pL}[A'_{1,+} + A'_{1,-}], \quad (26)$$

$$-\varepsilon_D De^{-kpL} = \varepsilon_1\{e^{-\gamma pL}[A_{1,+} - A_{1,-}] + e^{\gamma pL}[A'_{1,+} - A'_{1,-}]\}. \quad (27)$$

We now solve for $A_{i,-}$ in terms of $A_{i,+}$, and $A'_{i,-}$ in terms of $A'_{i,+}$, respectively. From Eqs. (17) and (18) we find

$$A_{1,-} = KA_{i,+}, \quad (28)$$

$$A'_{1,-} = K'A'_{1,+}, \quad (29)$$

where

$$K = -\frac{M_{11} - e^{-\gamma L}}{M_{12}},$$

$$K' = -\frac{M_{11} - e^{\gamma L}}{M_{12}}, \quad (30)$$

where $M_{i,j}$ is the (i,j) component of matrix M. Finally, by substituting Eqs. (28) and (29) into Eqs. (22), (23), (26), and (27), and after some algebra, we obtain

$$\begin{pmatrix} (1+K) & (1+K') & -1 & 0 \\ \varepsilon_A(1-K) & \varepsilon_A(1-K') & -\varepsilon_C & 0 \\ e^{-\gamma pL}(1+K) & e^{\gamma pL}(1+K') & 0 & -e^{-kpL} \\ \varepsilon_A e^{-\gamma pL}(1-K) & \varepsilon_A e^{\gamma pL}(1-K') & 0 & \varepsilon_D e^{-kpL} \end{pmatrix} \begin{pmatrix} A_{1,+} \\ A'_{1,+} \\ C \\ D \end{pmatrix} = 0. \quad (31)$$

The above system of equation admits a solution only if the determinant of the coefficient matrix vanishes. This finally leads us, after some algebra, to the following result:

$$[\varepsilon_A^2(1-K)(1-K') - \varepsilon_C\varepsilon_D(1+K)(1+K') - \varepsilon_A(\varepsilon_C - \varepsilon_D) \times (1-KK')]\tanh(\gamma pL) - \varepsilon_A(\varepsilon_C + \varepsilon_D)(K-K') = 0. \quad (32)$$

Equations (20) and (32) construct the implicit dispersion relation of IF phonons in the active region. All the solutions should satisfy simultaneously Eqs. (20) and (32). Once more, we can find, when one stage contains only two layers ($N=2$), Eq. (32) completely agrees with Eq. (45) in Ref. 27. The agreement demonstrates that the dispersion relation in a finite superlattice, derived by Camley *et al.*,[27] is a natural result of our model. In fact, we expand their model to a more general case in which one stage (period) is allowed to contain an arbitrary number of layers.

TABLE I. Dielectric constants and phonon frequencies used in the dispersion relation calculation (Ref. 19).

	GaAs	$Al_xGa_{1-x}As$
ε_∞	10.89	$10.89-2.73\times x$
$\hbar\omega_{LO}$ (GaAs-like) (meV)	36.25	$36.25-6.55\times x+1.79\times x^2$
$\hbar\omega_{TO}$ (GaAs-like) (meV)	33.29	$33.29-0.64\times x-1.16\times x^2$
$\hbar\omega_{LO}$ (AlAs-like) (meV)		$44.63+8.78\times x-3.32\times x^2$
$\hbar\omega_{TO}$ (AlAs-like) (meV)		$44.63+0.55\times x-0.30\times x^2$

III. NUMERICAL CALCULATION AND DISCUSSION

In this section, by using our model and transfer matrix model, respectively, we will present the dispersion relation and electrostatic potential of IF phonons in the active region of a quantum cascade laser. The following detailed discussion answers the two questions given in the Introduction. We take the QCL structure proposed by Hu *et al.* as an example.[28] The active region in this laser structure is composed by GaAs as quantum well and $Al_{0.15}Ga_{0.85}As$ as quantum barrier. Each stage consists of eight layers, and the layer sequence given in nanometers is **5.4**/7.8/**2.4**/6.4/**3.8**/14.8/**2.4**/9.4. $Al_{0.15}Ga_{0.85}As$ barriers are in boldface. Without loss of generality, we assume the active region contains ten stages and the up and down waveguide layers are composed by $Al_{0.15}Ga_{0.85}As$. Following the generalized Lyddane-Sachs-Teller relation, the dielectric function for binary and ternary compound semiconductors can be expressed as follows: for the binary semiconductor

$$\varepsilon(\omega) = \varepsilon(\infty)\frac{\omega^2 - \omega_{LO}^2}{\omega^2 - \omega_{TO}^2}$$

and for the ternary semiconductor

$$\varepsilon(\omega) = \varepsilon(\infty)\frac{(\omega^2 - \omega_{LO1}^2)(\omega^2 - \omega_{LO2}^2)}{(\omega^2 - \omega_{TO1}^2)(\omega^2 - \omega_{TO2}^2)},$$

where LO (TO) stands for the longitudinal (transverse) optical mode, and 1 and 2 denote material types. The dielectric constants and phonon frequencies used in this work are listed in Table I.

First we present the results of the transfer matrix model. Figure 2 shows the dispersion relation of IF phonons in the active region. There are 24 IF modes in total, including 16 GaAs-like and eight AlAs-like modes. The potential distributions of the eight AlAs-like modes in one stage, in the case $kL=5$, are given in Fig. 3. For an arbitrary IF mode, using the transfer matrix model to calculate the potential distribution in two adjacent stages, respectively, it is easy to find that the electrostatic potential $\Phi(z)$ is discontinuous at the interface of two stages. For example, Fig. 4 shows the potential distribution of the fifth AlAs-like mode in two adjacent stages. Obviously, the discontinuity cannot be neglected. We note, in other QCL structures, the discontinuity always exists in the distribution of phonon potential calculated by the transfer matrix model.[23–25] This obviously contradicts Laplace's equation and the boundary conditions. These re-

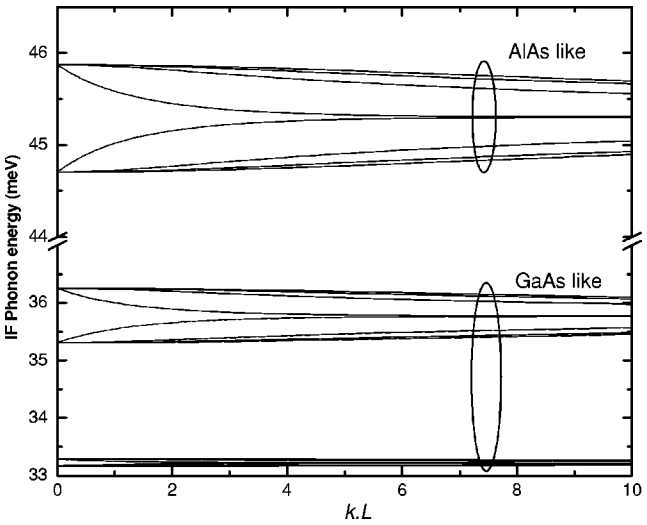

FIG. 2. Dispersion relation of IF phonons by transfer matrix model, where k is the in-plane wave vector and L is the length of one stage.

sults not only demonstrate that transfer matrix model cannot be directly used to deal with the IF modes in the active region, but strongly indicate that each stage cannot be considered as an isolated system.

We now present the phonon potential and the dispersion relation calculated by our model. Our results show that there are $3N(p+1)$ IF phonons in the active region, including $2N(p+1)$ GaAs-like modes and $N(p+1)$ AlAs-like modes. The dispersion relations of the latter are given in Fig. 5. Among the $N(p+1)$ AlAs-like modes, there are Np bulk modes for which γ is purely imaginary ($\mathrm{Re}[\gamma]=0$). The dispersion curves of the bulk modes are plotted by solid lines in Fig. 5. As is shown in Fig. 5, the dispersion curves of bulk modes construct N quasicontinuous subbands, each of which consists of p curves. Compared to Fig. 2, we can find the N discrete dispersion curves for AlAs-like modes in Fig. 2 turn

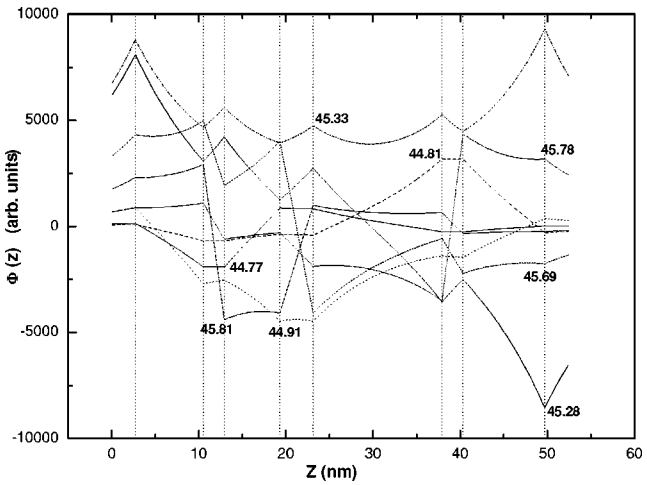

FIG. 3. IF phonon potential for eight AlAs-like modes in the case of $kL=5$, calculated by the transfer matrix model. Each mode is labeled with its energy in meV, and the vertical lines represent the interfaces between the layers in one stage.

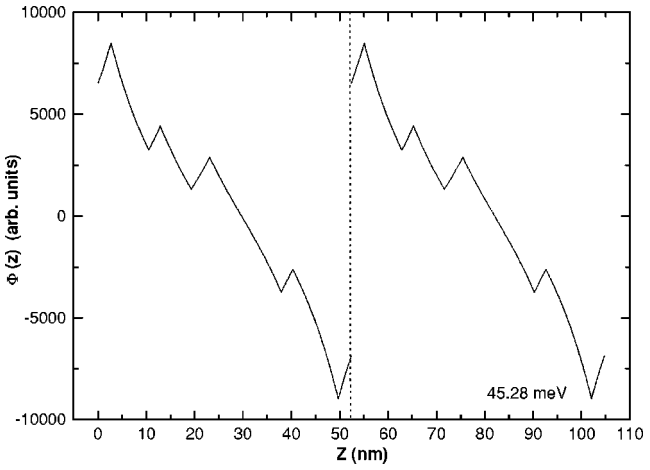

FIG. 4. Potential distribution of the fifth AlAs-like mode in two adjacent stages for $kL=5$, calculated by the transfer matrix model. The vertical dashed line represents the edge of one stage.

into N quasicontinuous subbands in Fig. 5. The reason is that in the transfer matrix model each stage is considered solitarily whereas in our model all the stages are considered and therefore the interaction between the stages is taken into account. Moreover, Fig. 5 also shows that there are N surface modes ($\mathrm{Re}[\gamma]>0$), corresponding to the dispersion curves plotted by scatters. From the inset of Fig. 5 we can find the energy of surface modes always locates in the gaps between the subbands of bulk modes.

Now we investigate the phonon potential of the bulk modes and surface modes. For the p bulk modes in the fourth

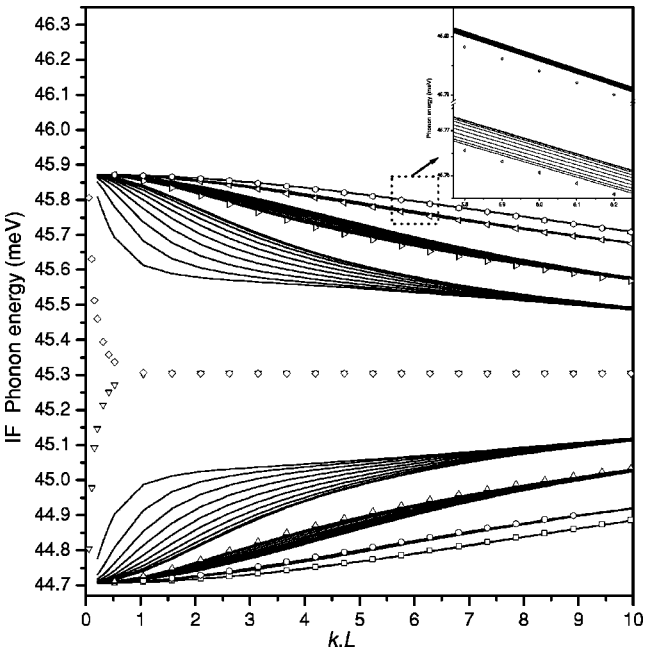

FIG. 5. Dispersion curves for AlAs-like IF phonons in the active region, calculated by our model. The bulk modes and surface modes are shown with solid lines and scatters, respectively. The inset shows that the dispersion curves of surface modes always locate in the gaps of the quasicontinuous subbands of bulk modes.

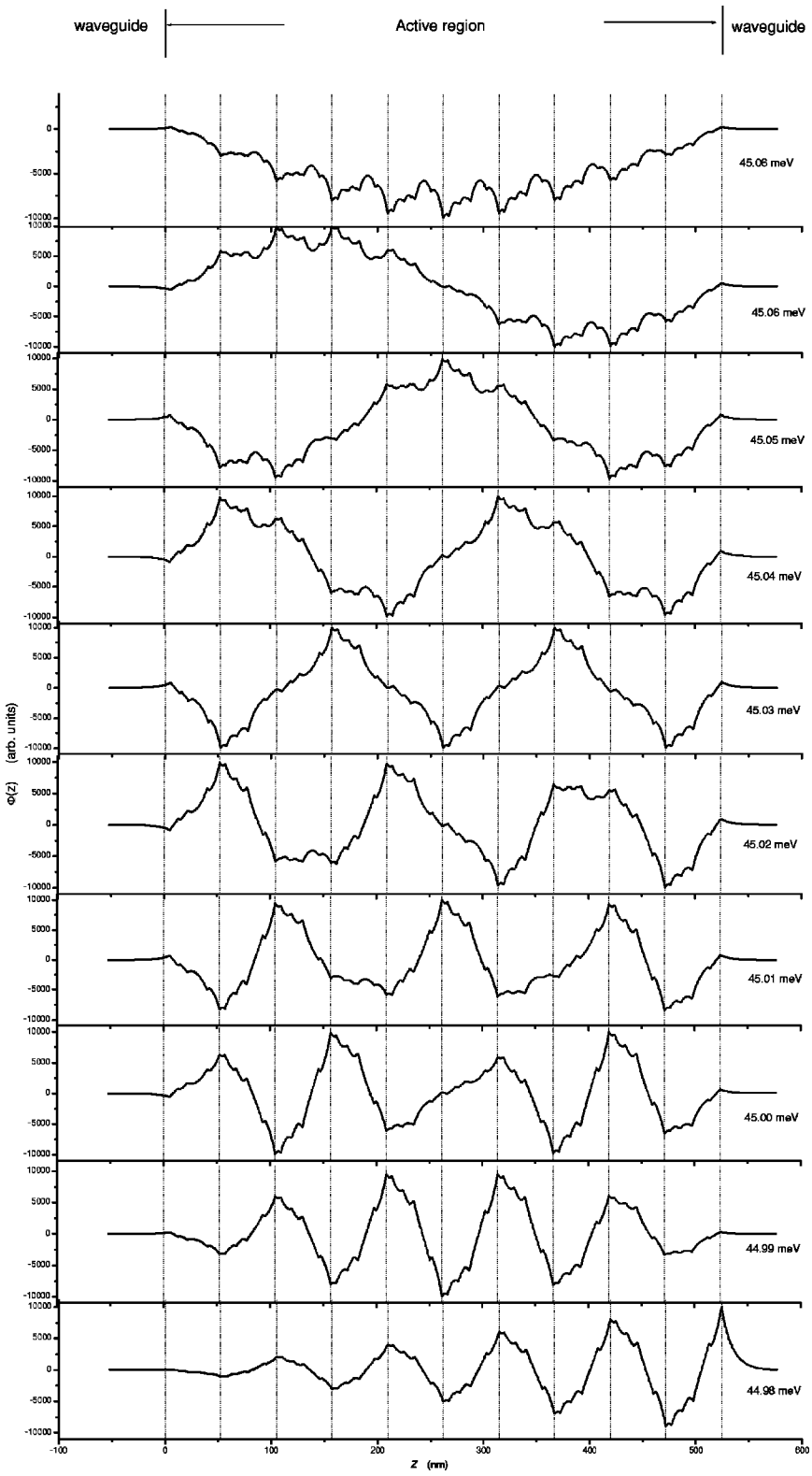

FIG. 6. Electrostatic potential generated by P bulk modes in the fourth subband for $kL=5$. Each mode is labeled with its energy. The vertical dashed lines represent the interfaces between the stages, as well as the interfaces between the active region and the waveguide layers.

subband (the energy of these bulk modes is about 45.0 meV in the short wavelength limitation), we calculate the distribution of their phonon potentials for the case $kL=5$. The results are given in Fig. 6. Obviously, the discontinuity of the phonon potential, which cannot be avoided in the transfer matrix model, is overcome in our model. Another important characteristic of bulk modes shown in Fig. 6 is that in the active region, the phonon potentials propagate in the form of Bloch waves with different wave vectors γ. Although the electrostatic potential of bulk modes propagates in an oscillation manner, the amplitude of the potential increases up to its maximum at each interface and decays away from each interface. This feature is consistent with the definition of the IF phonon. On the other hand, Fig. 7 gives the potential distri-

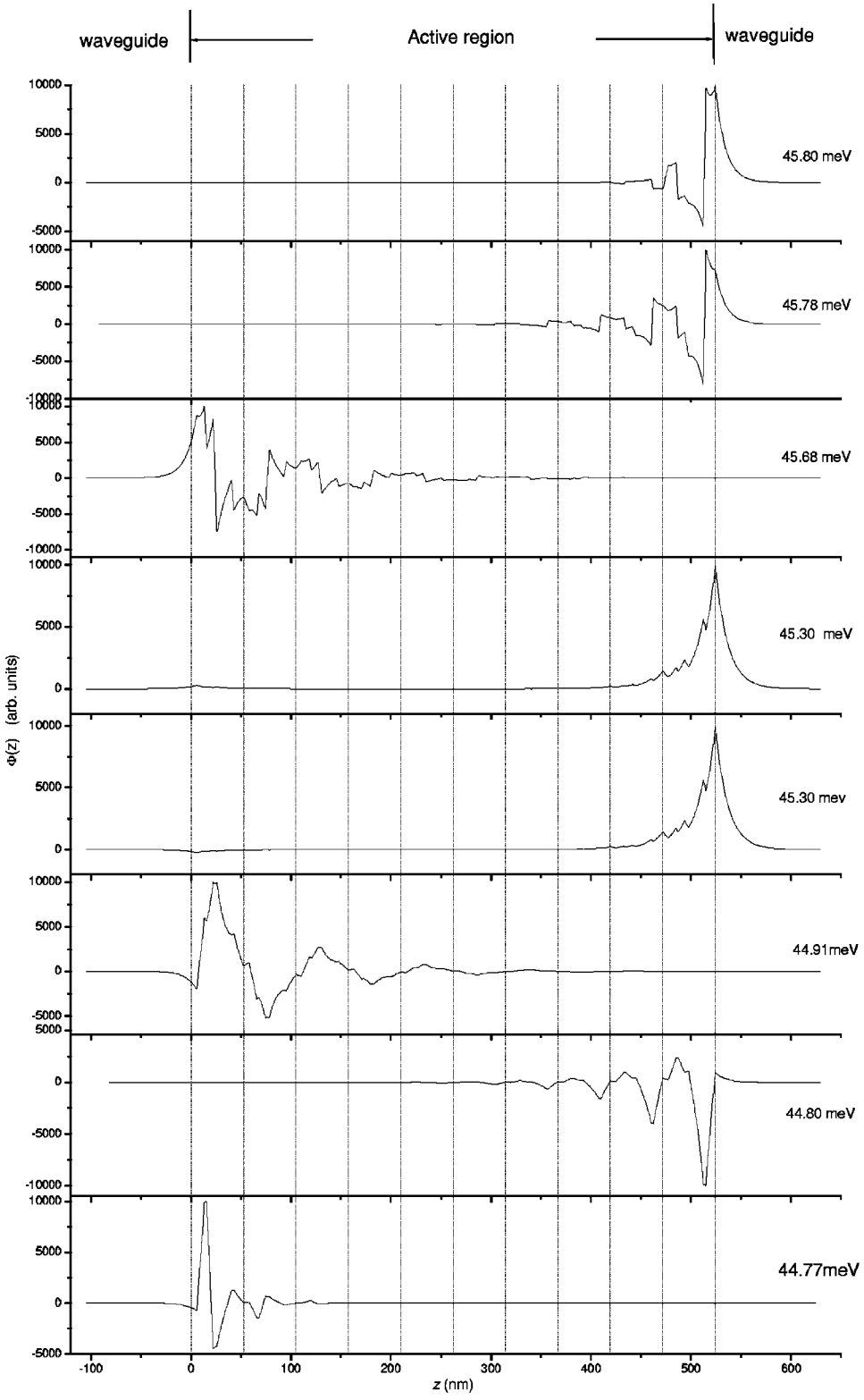

FIG. 7. Electrostatic potential generated by N surface modes for $kL=5$. Each mode is labeled with its energy. The vertical dashed lines represent the interfaces between the stages, as well as the interfaces between the active region and the waveguide layers.

bution of N surface modes. Figure 7 makes clear that the amplitudes of the surface modes localize in the vicinity of the interface between the active region and one of the waveguide layers, and decay quickly away from the interface. It is worth noticing that these two kinds of modes were found theoretically in a finite superlattice,[27,29–31] and then detected in a GaAs/AlAs finite superlattice by Raman scattering and high-resolution electron-energy-loss spectroscopy.[32,33] Our work indicates that these modes commonly exist in finite periodic systems.

A common character shown in Figs. 6 and 7 is that the distribution of phonon potentials in various stages is significantly different. As seen in Fig. 6, comparing the distribution of phonon potentials in the outmost stage with the center

stage, we observe significant differences in the amplitude and the profile of the potential. Furthermore, the existence of surface modes makes the character clearer. This character answers the questions proposed in the Introduction of this paper. To summarize, interaction between the stages cannot be neglected and the distribution of the phonon potential is significantly different in various stages.

IV. CONCLUSIONS

We have proposed a model to describe the electrostatic potential and the corresponding dispersion relation of the IF phonons in the active region of quantum cascade lasers. Our model takes into account all the stages and the interaction between them. Our model agrees with the model for finite superlattice, but can be applied in more general cases where one stage (period) is allowed to contain an arbitrary number of layers. In addition, we prove that the transfer matrix model cannot be used directly, because it fails to keep the phonon potential continuous at the interface of adjacent stages.

Numerical calculations of our model show that the IF phonons in the active region can be classified into bulk modes and surface modes. The dispersion curves of the bulk modes construct a series of quasicontinuous subbands, and the phonon potentials propagate in an oscillating manner inside the active region. The dispersion curves of surface modes locate in the gaps between the subbands of the bulk modes. The phonon potentials of surface modes localize in the vicinity of the interface between the active region and one of the waveguide layers, and decay fast away from the interface. Our results point out that the distribution of the phonon potential in various stages is significantly different, and the interaction between the stages cannot be neglected.

To sum up, we provide a complete picture of the IF phonon spectra in a practical quantum cascade laser. The electrostatic potential and the dispersion relation obtained by our model can be directly used to calculate the electron-IF phonon scattering rates in QCL structure. This study is essential for accurately evaluating the electron transport properties in QCLs, and is therefore needed to achieve best performance QCLs and other intersubband lasers or detectors.

ACKNOWLEDGMENTS

This work is supported by the National High Technology Research and Development Program of China (Grant No. 2001AA311150), National Natural Sciences Foundation of China (Grant Nos. 60136010 and 60406008), and 973 Program of China (Grant No. G200068302).

[1] J. Faist, F. Capasso, D. L. Sivco, C. Sirtori, A. L. Hutchinson, and A. Y. Cho, Science **264**, 553 (1994).
[2] C. Sirtori, P. Kruck, S. Barbieri, P. Collot, J. Nagle, M. Beck, J. Faist, and U. Oesterle, Appl. Phys. Lett. **73**, 3486 (1998).
[3] R. Kohler, A. Tredicucci, F. Beltram, H. E. Beere, E. H. Linfield, A. G. Davies, D. A. Ritchie, R. C. Iotti, and F. Rossi, Nature (London) **417**, 156 (2002).
[4] J. S. Yu, S. Slivken, A. Evans, L. Doris, and M. Razaghi, Appl. Phys. Lett. **83**, 2503 (2003).
[5] J. Faist, F. Capasso, C. Sirtori, D. L. Sivco, A. L. Hutchinson, M. S. Hybertsen, and A. Y. Cho, Phys. Rev. Lett. **76**, 411 (1996).
[6] G. Strasser, S. Gianordoli, L. Hvozdara, W. Schrenk, K. Unterrainer, and E. Gornik, Appl. Phys. Lett. **75**, 1345 (1999).
[7] B. S. Williams, S. Kumar, H. Callebaut, Q. Hu, and J. L. Reno, Appl. Phys. Lett. **83**, 2124 (2003).
[8] J. Faist, F. Capasso, C. Sirtori, D. L. Sivco, and A. Y. Cho, *Intersubband Transitions in Quantum Wells: Physics and Device Applications II*, edited by H. C. Liu and F. Capasso, Semiconductors and Semimetals Vol. 66 (Academic, New York, 2000), Chap. 1.
[9] J. H. Smet, C. G. Fonstad, and Q. Hu, J. Appl. Phys. **79**, 9305 (1996).
[10] K. Donovan, P. Harrison, and R. W. Kelsall, J. Appl. Phys. **89**, 3084 (2001).
[11] F. Compagnone, A. Di Carlo, and P. Lugli, Phys. Rev. B **65**, 125314 (2002).
[12] M. A. Stroscio, M. Kisin, G. Belenky, and S. Luryi, J. Appl. Phys. **75**, 3258 (1999).
[13] K. W. Kim, A. R. Bhatt, M. A. Stroscio, P. J. Turley, and S. W. Teisworth, J. Appl. Phys. **72**, 2282 (1992).
[14] R. Chen, D. L. Lin, and T. F. George, Phys. Rev. B **41**, 1435 (1990).
[15] D. L. Lin, R. Chen, and T. F. George, Solid State Commun. **73**, 799 (1990).
[16] R. Lassnig, Phys. Rev. B **30**, 7132 (1984).
[17] K. Huang and B. Zhu, Phys. Rev. B **38**, 13377 (1988); **38**, 2183 (1988).
[18] N. Mori and T. Ando, Phys. Rev. B **40**, 6175 (1989).
[19] S. Yu, K. W. Kim, M. A. Stroscio, G. J. Iafrate, J. P. Sun, and G. I. Haddad, J. Appl. Phys. **82**, 3363 (1997).
[20] I. Lee, S. M. Goodnick, M. Gulia, E. Molinari, and P. Lugli, Phys. Rev. B **51**, 7046 (1995).
[21] H. Rucker, E. Molinari, and P. Lugli, Phys. Rev. B **45**, 6747 (1992).
[22] K. W. Kim, A. R. Bhatt, M. A. Stroscio, P. J. Turley, and S. W. Teitsorth, J. Appl. Phys. **72**, 2282 (1997).
[23] B. S. Williams and Q. Hu, J. Appl. Phys. **90**, 5504 (2001).
[24] V. M. Menon, W. D. Goodhue, A. S. Karakashian, and L. R. Ram-Mohan, J. Appl. Phys. **88**, 5262 (2000).
[25] M. V. Kisin, M. A. Stroscio, G. Belenky, V. B. Gorfinkel, and S. Luryi, J. Appl. Phys. **83**, 4816 (1998).
[26] R. E. Camley and D. L. Mills, Phys. Rev. B **29**, 1695 (1984).
[27] B. L. Johnson, J. T. Weiler, and R. E. Camley, Phys. Rev. B **32**, 6544 (1985).
[28] B. S. Williams, H. Callebaut, S. Kumar, Q. Hu, and J. L. Reno, Appl. Phys. Lett. **82**, 1015 (2003).

[29] T. Tsuruoka, Y. Uehara, and S. Ushioda, Phys. Rev. B **49**, 4745 (1994).
[30] W. M. Liu, G. Eliasson, and J. J. Quinn, Solid State Commun. **55**, 533 (1985).
[31] J. S. Nkoma, Surf. Sci. **191**, 595 (1987).
[32] A. K. Sood, J. Menendez, M. Cardona, and K. Ploog, Phys. Rev. Lett. **54**, 2115 (1985).
[33] T. Tsuruoka, M. Sekoguchi, Y. Uehara, S. Ushioda, T. Kojima, and K. Ohta, Phys. Rev. B **50**, 2346 (1994).